JMEPEG (2010) 19:1357–1361
DOI: 10.1007/s11665-010-9629-x

1059-9495/$19.00

Potentiodynamic Polarization Aspects of the As-cast and Sprayed Al-Si, Al-Sn and Al-Sn-Si Alloys in a Sodium Chloride Solution

M. Anil, S. Balaji, A. Upadhyaya, M.K. Ghosh, and S.N. Ojha

(Submitted September 1, 2008; in revised form January 25, 2010)

The present study compares the corrosion behavior of Al-Sn, Al-Si and Al-Sn-Si alloys processed by spray forming with that of the conventional chill cast ones in aqueous 0.1 N NaCl solution. Spray forming resulted in finer microstructural features with uniform distribution of second-phase particles. The spray formed Al-Si samples showed improved corrosion resistance as compared to the chill cast ones. The Sn containing alloys showed inferior corrosion resistance in the neutral electrolyte. The addition of 12.5 wt.% Si to Al-Sn alloys improves the corrosion resistance.

Keywords bearing alloys, corrosion, potentiodynamic polarization, chill casting, spray forming

1. Introduction

Al-based systems with Sn and Si additions possess good tribological and mechanical properties and are widely used in engineering applications, such as plain bearings, internal combustion engine pistons and cylinder liners (Ref 1). Although Al-Sn alloys exhibit good anti-frictional characteristics, they lack the ability to support heavy loads due to the soft nature of Sn. In contrast, Al-Si alloys exhibit excellent wear resistance due to the presence of hard Si phase. However, these alloys have poor seizure resistance. To overcome these problems, there has been an increasing trend of adding Si into Al-Sn alloys to improve their ability to support load and resistance to fatigue (Ref 2).

The processing of these alloys by conventional liquid metallurgy routes results in coarse grain microstructure with large degree of segregation of alloying elements. In recent years, spray forming process has proven to be effective in achieving better microstructural control (Ref 3). Rapid solidification effects, inherent in spray forming process due to high rate of heat transfer at the droplet gas interface and deposition surface, ensure considerable chemical and microstructural homogeneity of the spray deposit. Rapid solidification processing results in non-equilibrium structure and hence improves properties. In addition, spray forming is capable of producing refined and segregation-free structures by the modification of growth morphology of the constituent phases (Ref 4).

The influence of structural morphology of the microconstituents as a result of processing routes and solute distribution on the corrosion behavior has been reported by various researchers (Ref 5-9). Ośorio et al. (Ref 10) have demonstrated the effect of dendrite arm spacing and solute redistribution on the corrosion resistance of directionally solidified samples of Al-10wt.%Sn and Al-20wt.%Zn alloys. They have reported that coarser dendritic structure is beneficial in improving the corrosion performance of Al-Zn alloys, whereas a finer dendritic structure results in lower corrosion rates in Al-Sn alloys. Also, some contradictory results regarding the microstructural refinement on corrosion resistance were reported by earlier researchers (Ref 11-13). However, there is not much literature available on the corrosion response of the spray formed Al alloys in particular Al-Si-Sn alloys.

The present study investigates the effect of processing routes (spray forming and chill casting) on the corrosion behavior of Al-Sn, Al-Si binary alloys and Al-Sn-Si ternary alloy in aqueous 0.1 N NaCl solution. Potentiodynamic polarization studies were carried out on the spray formed Al-25wt.%Sn, Al-12.5wt.%Si, and Al-25wt.%Sn-12.5wt.%Si alloys and the corrosion behavior was compared with the conventional chill cast alloys of similar compositions.

2. Experimental Procedure

The nominal composition of the alloys used for corrosion studies were Al-25wt.%Sn, Al-12.5wt.%Si and Al-25wt.%Sn-12.5wt.%Si. Table 1 lists the chemical compositions of the base alloy ingots used for both spray forming and chill casting. The alloy ingots were melted in a graphite crucible under argon atmosphere in a resistance heating furnace. The temperature of the melt was measured within a variation of ±2 °C using a chromel-alumel thermocouple connected to a temperature recorder. Melt superheat of 200 °C was ensured in all the experiments to achieve homogeneity of the melt. The melt was

M. Anil and **M.K. Ghosh**, Department of Mechanical Engineering, Institute of Technology, Banaras Hindu University, Varanasi 221005, India; **S. Balaji** and **A. Upadhyaya**, Department of Materials and Metallurgical Engineering, Indian Institute of Technology Kanpur, Kanpur 208016, India; and **S.N. Ojha**, Department of Metallurgical Engineering, Institute of Technology, Banaras Hindu University, Varanasi 221005, India. Contact e-mail: anily2k@gmail.com.

Table 1 Chemical composition of base alloys (wt.%)

Alloy	Sn	Si	Fe	Mg	Zn	Mn	Al
Al-25Sn	25.1	0.01	0.02	<0.01	…	0.01	Balance
Al-12.5Si	…	12.49	0.14	…	0.01	<0.01	Balance
Al-25Sn-12.5Si	24.93	12.51	0.15	<0.01	0.01	0.01	Balance

Table 2 Tafel extrapolation data for both chill-cast and spray-formed Al-alloys

	E_{corr}, mV		i_{corr}, 10^{-6} A/cm^2		Corrosion rate, mmpy	
Composition	Chill cast	Spray formed	Chill cast	Spray formed	Chill cast	Spray formed
Al-12.5Si	−656	−712	2.492	0.96	0.027	0.01
Al-25Sn	−895	−1160	12.58	37.44	0.148	0.44
Al-25Sn-12.5Si	−885	−857	4.46	6.26	0.051	0.053

atomized employing a convergent-divergent nozzle into a spray of micron-sized droplets, using nitrogen as an inert gas at an atomization pressure of 1.0 MPa. In this process, high-velocity gas jet interacts with liquid stream at the tip of the flow tube, centered concentrically in the gas flow channel of the nozzle, and disintegrates the liquid into fine droplets. The spray of droplets was collected over a copper substrate at a deposition distance of 350 mm, leading to a bell-shaped bulk deposit. The details of the spray deposition process employed in the present work have been described elsewhere (Ref 14). In another set of experiment, cylindrical-shaped chill cast samples were produced by pouring the melt at 750 ± 4 °C into a cast iron mould. The samples for corrosion studies were collected from the central region of the spray deposited perform and core of the chill cast alloys.

The electrochemical evaluation was carried out in a freely aerated 0.1 N NaCl (pH value: 6.8) solution at a constant scan rate of 1 mV/s at room temperature using a flat cell with standard three-electrode (reference, counter, and working) configuration. The reference electrode used for the present experiment was calomel electrode (SCE) saturated with saturated KCl and the polished surface of the sample under investigation was chosen as the working electrode. A platinum mesh acted as a counter electrode. The potentiodynamic polarization scans were performed using potentiostat (model: PC4; supplier: Gamry Instruments, Inc., USA). All polarization tests were repeated three times to verify the accuracy and to confirm the final results. Prior to the polarization test, each sample was stabilized for about 3600 s in the solution in order to obtain a stable open circuit potential (OCP). From the polarization curves i_{corr} was measured by the Tafel extrapolation (i.e., extrapolating the linear segments of the cathodic and the anodic curves). The extrapolation results obtained from the polarization curves are summarized in Table 2. From the value of i_{corr} the corrosion rate is calculated using the following expression:

$$\text{Corrosion rate (mmpy)} = 0.0033 \times \frac{e}{\rho} \times i_{corr} \qquad \text{(Eq 1)}$$

where e is the equivalent weight, ρ is the density, and i_{corr} is the corrosion current.

3. Results and Discussion

Figure 1 shows the microstructural differences between the spray-formed and chill-cast samples**.** In Fig. 1(a), the micrograph of spray formed Al-12.5Si alloy revealing a uniform distribution of fine globular-shaped eutectic Si phase, with a size in the range of 1-3 μm, within Al matrix is evident. Whereas coarse needle and flake-like eutectic Si appeared in the cast alloy. Figure 1(b) shows the micrographs of Al-25Sn alloy, indicating dendritic and equiaxed grain morphologies of the primary α-phase for cast and spray formed alloys respectively. In Fig. 1(c), the microstructure of the spray formed Al-12.5Si-25Sn is showing a highly refined eutectic Si phase in dark gray contrast and Sn in light gray contrast. The eutectic Si and Sn are uniformly distributed within the Al-matrix. At some places, Sn seems to nucleate either at the Si surface or fully envelope the Si particles. These features are in contrast to those in the cast alloy which show both dendritic needle-like Si and platelet-shaped Si particles with a maximum size of 30 μm.

The Al-Sn alloy system is an immiscible binary system with a solid solubility limit of Al lies below 0.09 wt.% Sn (0.02 at.% Sn) (Ref 15, 16). Therefore, Al-Sn alloys, with higher Sn contents (above 0.09 wt.%), are form two kinds of structures: either as 'a continuous network of Sn at grain boundaries of Al solution' or as 'Sn particles distributed uniformly over a continuous Al-rich matrix' solely based on the mode of solidification. The microstructural features generally observed with spray-formed materials are due to the rapid solidification effect achieved during atomization and deposition stages of the process. In addition, high-impact velocity of the droplets and the turbulent fluid flow conditions on the growing deposit also give rise to fragmentation of dendrite arms and thus the refinement of the primary phases and homogeneity in the microstructure (Ref 17-19). The last solidifying phase Sn is segregated at the grain boundaries of primary α-Al phase along with eutectic Si in the cast Al-Si-Sn alloy (Ref 2). In addition, Sn content is high at chilled zones rather than other portion of cast ingots due to inverse segregation (Ref 20). However, during spray deposition, a turbulent condition on the deposit surface gives rise to refinement of Sn particles. The high temperature in the preform after deposition leads to segregation

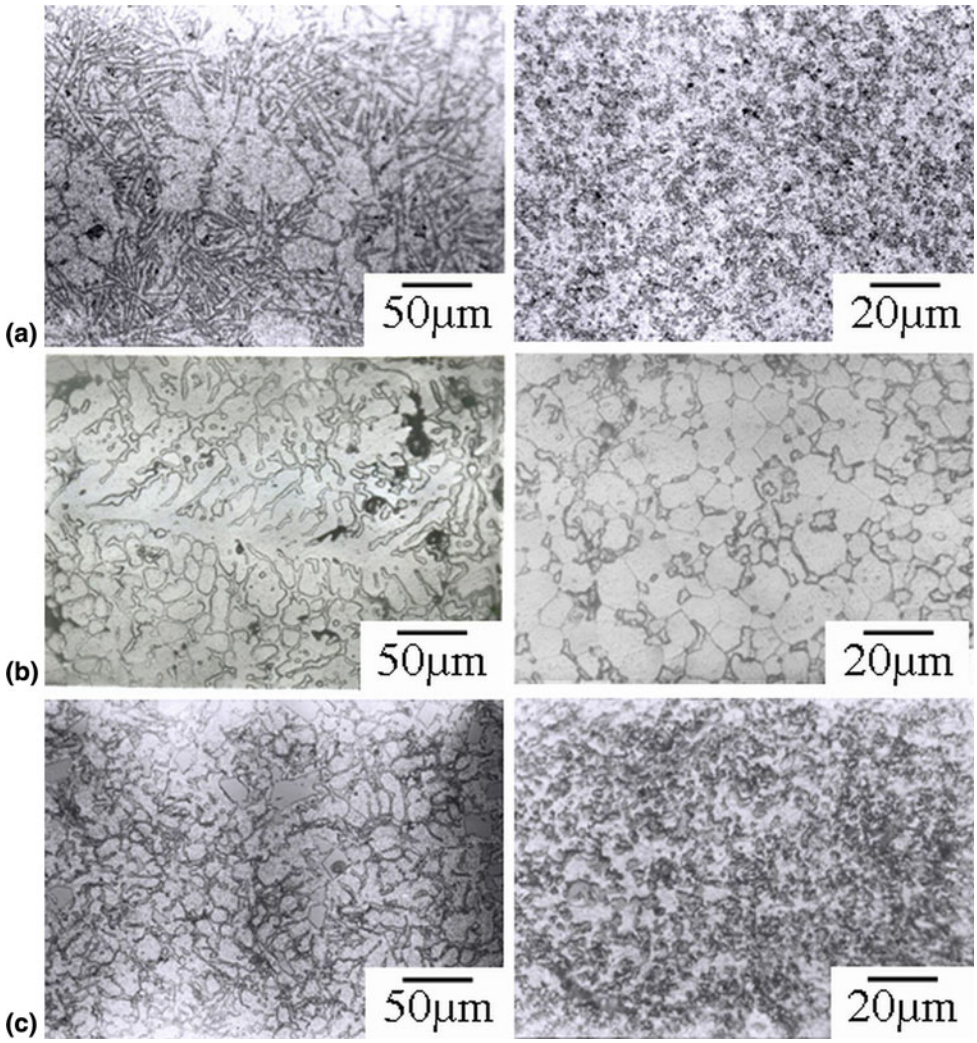

Fig. 1 Optical micrographs of (a) Al-12.5wt.%Si, (b) Al-25wt.%Sn and (c) Al-25wt.%Sn-12.5wt.%Si alloys processed by conventional chill casting (left) and spray forming (right)

of Sn on Si phase. Whereas a moderately high cooling rate in the deposit does not allow full segregation of Sn around the Si particles. It is therefore concluded that a highly refined microstructural feature is obtained during spray forming that constitutes uniform distribution of Sn in Al matrix.

The variation of open circuit potential with time for both spray-formed as well as chill-cast samples in 0.1 N NaCl solution is shown in Fig. 2. The stabilization of OCP occurs immediately after immersion of all compositions investigated except Al-25Sn alloy. There is no appreciable change in the OCP values between the spray-formed samples and the chill-cast ones. However, a drop of about 200 mV in OCP is observed for the Sn-added sample as compared to the Al-12.5Si alloy.

The cathodic and anodic polarization scans for the chill-cast as well as spray-formed samples of Al-25Sn, Al-25Sn-12.5Si and Al-12.5Si are given in Fig. 3. None of the samples exhibited active-passive transition in 0.1 N NaCl environment. Al in neutral pH is known to possess stable passive film (Ref 21) and is therefore quite likely the reason for no active-passive behavior noticed as Al is the primary phase (OCP falls in the passive region). The kinks in the curves indicate pit formation that is also evident from the micrographs. Pitting represents the most common form of corrosion for Al alloys particularly in solutions containing chloride ions (Ref 22).

The E_{corr} values reported in Table 2 followed the same trend as that of the open circuit potentials. Higher value of E_{corr} observed for the Al-Si alloy is a thermodynamic indication of nobler behavior than that of the Al-Sn alloy. Addition of Si to the Al-25Sn alloy results in nobler E_{corr} values than those of Al-25Sn alloys and hence suggests an improvement in corrosion resistance. From the micrographs of corroded alloy shown in Fig. 4, it is evident that the attack has been initiated at the Al-Si interface on the Al phase. This could be attributed to the possible formation of galvanic coupling between Al and Si phases. As Al is more active (−1.66 V versus SHE) than Si (−0.9 V versus SHE), Al acts as anode and corrodes preferentially. Elsewhere, Fratila-Apachitei et al. (Ref 23) have reported the possibility of galvanic coupling at the Al-Si interface on the basis of scanning Kelvin probe force microscopy studies conducted on Al-10wt.%Si alloy. Osorio et al. (Ref 12, 13) also reported the occurrence of localized (galvanic) corrosion in case of Al-Si cast alloys. And also mentioned that 'although Si is nobler than Al, Si particle grows from the liquid

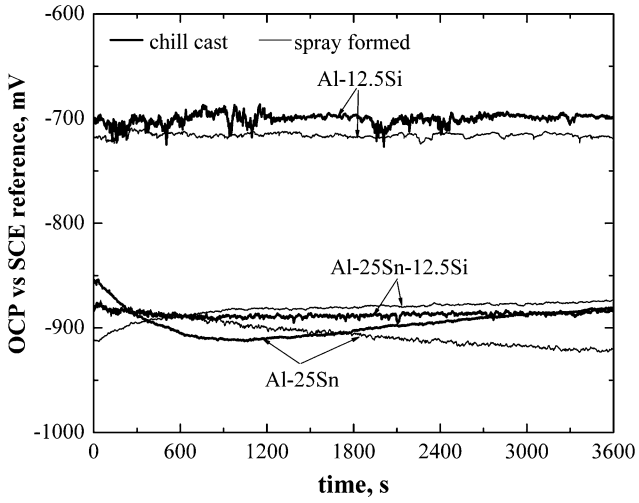

Fig. 2 Open circuit potential stabilization curves for spray-formed and chill-cast Al alloys

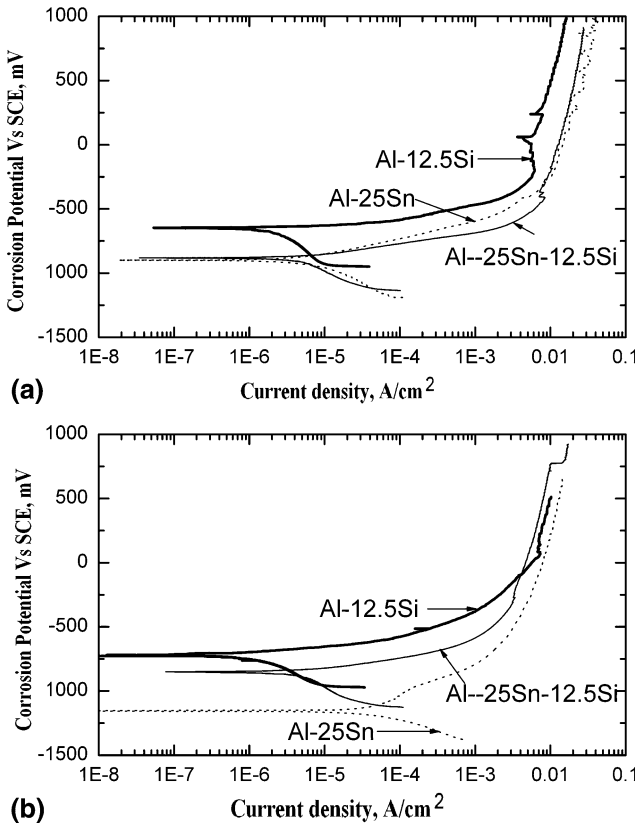

Fig. 3 Potentiodynamic polarization curves for the Al alloys processed by (a) chill casting and (b) spray forming

in a faceted manner (smooth growth interface) while the Al-rich phase solidifies with surfaces that are rough'. These dissimilarities in growth behavior lead to localized deformations at Al-Si interface. Further, such localized deformation between Al (rough) and Si particle (smooth) could be more susceptible to corrosion when compared with the 'Al-rich matrix regions which are not close to the Si particles (minimizing the galvanic cell effect)'.

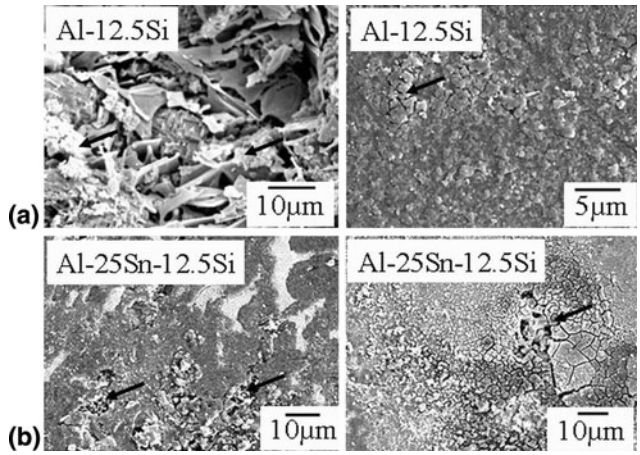

Fig. 4 Corroded microstructures of (a) Al-Si and (b) Al-Si-Sn alloys processed by chill casting (left) and spray forming (right). The *arrow mark* shows the corroded regions

When galvanic coupling is the main cause of corrosion, the area ratio between noble and less-noble phases is one of the key factors in determining the severity of corrosion (Ref 24). As shown in Fig. 4(a), the severity of the attack is less for spray-formed alloys in comparison with chilled-cast alloys which lead to less i_{corr} values and hence exhibited lower corrosion rate. This could be attributed to the extended solid solubility of second phase in Al phase, which is a common phenomenon in rapid solidification process. Together this solid-solubility is accompanied by microstructural refinement of both eutectic Si and eutectic Al. The enhanced corrosion resistance of Al-Si alloy with spray-forming process is therefore believed to be associated with the reduced effective area ratio between these two phases compared to that of the chill cast counterpart.

From the Tafel extrapolation data reported in Table 2, it is evident that addition of Sn decreases the corrosion resistance. Elsewhere, Kliskic et al. (Ref 25) also reported that the corrosion resistance decreased with increasing Sn content. The presence of alloying elements such as Sn produces some point defects in the oxide layer (Al_2O_3). In neutral solutions, Sn has been reported to be in passive state. In the neutral pH solutions, both Stannous oxide and Stannic oxide can coexist as the potential difference between the two equilibria is just 2 mV. Elsewhere, the presence of both Sn^{2+} and Sn^{4+} ions in the oxide layer of the Al-3wt.%Sn alloy in 3.5 wt.% NaCl solution has been confirmed by XPS studies as well (Ref 26). The incorporation of these ions into the Al_2O_3 film increases the anionic as well as cationic vacancies. These defects help the aggressive ions such as Cl^- ions to reach the metal/metal-oxide interface and thereby lead to the thinning of the oxide film and bulk metal (Al) corrosion. The thinning of the oxide film accounts for the lowering of the OCP as well as corrosion resistance of the Sn-added Al alloys.

The addition of 12.5wt.%Si to Al-25wt.%Sn alloy decreases the corrosion rate. The improved corrosion behavior of Al-25wt.%Sn-12.5wt.% Si alloy as compared to that of Al-25wt.%Sn alloy can be attributed to the possible incorporation of Sn in SiO_2 structure as Sn^{4+} that leads to decrease in defect concentration of the oxide layer.

The Sn-containing alloys produced by chill casting showed better corrosion resistance than those produced by

spray-forming process. One of the major possible reasons apart from other metallurgical aspects (cooling rate, immiscibility of Sn in Al lattice, ternary eutectic, dendrite spacings into the eutectic ternary lattice, etc.) might be the variation of Sn content in the cast samples unlike the spray-formed ones. As the samples were selected from the core of the cylindrical chill-cast alloys, the Sn content might be lower than the nominal composition because of the inverse segregation (Ref 20) effect. Whereas spray-formed liquid-phase-immiscible alloys in earlier studies were also reported uniform distribution of second-phase elements (Ref 17-19).

4. Conclusions

- Al-Si alloys show better corrosion resistance irrespective of the processing routes. Spray-formed Al-Si alloys possess better corrosion resistance in comparison to chill-cast Al-Si alloys.
- The addition of Si to the Al-Sn alloy system improves the corrosion resistance.

Acknowledgment

The authors gratefully acknowledge the assistance from E.R. Tagore (IIT Kanpur) with the electrochemical characterization experiments.

References

1. B.K. Prasad, K. Venkateswarlu, O.P. Modi, and A.H. Yegneswaran, Influence of the Size and Morphology of Silicon Particles on the Physical, Mechanical and Tribological Properties of Some Aluminium–Silicon Alloys, *J. Mater. Sci. Lett.*, 1996, **15**, p 1773–1776
2. G.C. Yuan, Z.J. Li, Y.X. Lou, and X.M. Zhang, Study on Crystallization and Microstructure for New Series of Al-Sn-Si Alloys, *Mater. Sci. Eng. A*, 2000, **280**, p 108–115
3. M. Anil and S.N. Ojha, Spray Processing and Wear Characteristics of Al-Cu-Al_2O_3-Pb Based Composites, *J. Mater. Sci.*, 2006, **41**, p 1073–1080
4. S.C. Lim, M. Gupta, Y.F. Leng, and E.J. Lavernia, Wear of a Spray-Deposited Hypereutectic Aluminium-Silicon Alloy, *Mater. Processing Tech.*, 1997, **63**, p 865–870
5. K.G. Watkins, M.A. McMahon, and W.M. Steen, Microstructure and Corrosion Properties of Laser Surface Processed Aluminium Alloys: A Review, *Mater. Sci. Eng. A*, 1997, **231**, p 55–61
6. I. Garcia and J.J.D. de Damborenea, Corrosion Properties of Tin Prepared by Laser Gas Alloying of Ti and Ti-6Al-4V, *Corros. Sci.*, 1998, **40**, p 1411–1419
7. G. Song, A.L. Bowles, and D.H. St John, Corrosion Resistance of Aged Die-Cast Magnesium Alloy AZ91D, *Mater. Sci. Eng. A*, 2004, **366**, p 74–86
8. G. Song, Recent Progress in Corrosion and Protection of Magnesium Alloys, *Adv. Eng. Mater.*, 2005, **7**, p 563–586
9. F.A. Davis and T.S. Eyre, The Effect of Silicon Content and Morphology on the Wear of Aluminium-Silicon Alloys Under Dry and Lubricated Sliding Conditions, *Tribol. Int.*, 1994, **27**, p 171–181
10. W.R. Ośorio, J.E. Spinelli, N. Cheung, and A. Garcia, Secondary Dendrite Arm Spacing and Solute Redistribution Effects on the Corrosion Resistance of Al-10 wt.%Sn and Al-20 wt.% Zn Alloys, *Mater. Sci. Eng. A*, 2006, **420**, p 179–186
11. S. Virtanen, H. Böhni, R. Busin, T. Marchione, M. Pierantoni, and E. Blank, The Effect of Laser Surface Modification on the Corrosion Behaviour of Fe and Al Base Alloys, *Corros. Sci.*, 1994, **36**, p 1625
12. W.R. Osorio, P.R. Goulart, G.A. Santos, M.N. Carlos, and A. Garcia, Effect of Dendritic Arm Spacing on Mechanical Properties and Corrosion Resistance of Al-9 wt% Si and Zn-27 wt% Al Alloys, *Metall. Mater. Trans.*, 2006, **37**, p 2525–2538
13. W.R. Osorio, N. Cheung, J.E. Spinelli, K.S. Cruz, and A. Garcia, Microstructural Modification by Laser Surface Remelting and its Effect on the Corrosion Resistance of an Al 9 wt% Si Casting Alloy, *Appl. Surf. Sci.*, 2008, **254**, p 2763–2770
14. S.N. Ojha, O.P. Pandey, B. Tripathi, M. Kumar, and C. Ramachandra, Microstructure and Wear Characteristics of an Al–4Cu–20Pb Alloy Produced by Spray Deposition, *Mater. Trans. JIM*, 1992, **33**, p 519–524
15. M. Hansen, *Constitution of Binary Alloy*, McGraw-Hill, New York, 1958, p 135
16. A. Perrone, A. Zocco, H. de Rosa, R. Zimmermann, and M. Bersani, Al–Sn Thin Films Deposited by Pulsed Laser Ablation, *Mater. Sci. Eng. C*, 2002, **22**, p 465–468
17. G.B. Rudrakshi, V.C. Srivastava, J.P. Pathak, and S.N. Ojha, Spray Forming of Al–Si–Pb Alloys and Their Wear Characteristics, *Mater. Sci. Eng. A*, 2004, **383**, p 30–38
18. G.B. Rudrakshi, V.C. Srivastava, and S.N. Ojha, Microstructural Development in Spray Formed Al–3.5Cu–10Si–20Pb Alloy and Its Comparative Wear Behaviour in Different Environmental Conditions, *Mater. Sci. Eng. A*, 2007, **457**, p 100–108
19. G.B. Rudrakshi and S.N. Ojha, Spray Forming and Wear Characteristics of Liquid Immiscible Alloys, *J. Mater. Process. Technol.*, 2007, **189**, p 224–230
20. K.S. Cruz, I.L. Ferreira, J.E. Spinelli, N. Cheung, and A. Garcia, Inverse Segregation During Transient Directional Solidification of Al-Sn Alloys: Numerical and Experimental Analysis, *Mater. Chem. Phys.*, 2009, **115**, p 116–121
21. M. Pourbaix, *Atlas of Electrochemical Equilibria in Aqueous Solutions*, NACE, Houston, TX, 1974
22. S. Wernick, R. Pinner, and P.G. Sheaby, *The Surface Treatment and Finishing of Aluminium and its Alloys*, 5th ed., ASM, Metals Park, OH, 1987
23. L.E. Fratila-Apachitei, I. Apachitei, and J. Duszczyk, Characterization of Cast AlSi(Cu) Alloys by Scanning Kelvin Probe Force Microscopy, *Electrochim. Acta*, 2006, **51**, p 5892–5896
24. C. Park, S. Kim, Y. Kwon, Y. Lee, and J. Lee, Mechanical and Corrosion Properties of Rheocast and Low-Pressure Cast A356–T6 Alloy, *Mater. Sci. Eng. A*, 2005, **391**, p 86–94
25. M. Kliskic, J. Radosevic, S. Gudic, and M. Smith, Cathodic Polarization of Al-Sn Alloy in Sodium Chloride Solution, *Electrochim. Acta*, 1998, **43**, p 3241–3255
26. P. Venugopal, P. Veluchamy, P. Selvam, H. Minoura, and V.S. Raja, X-Ray Photoelectron Spectroscopic Study of the Oxide Film on an Aluminium-Tin Alloy in 1.5% Sodium Chloride Solution, *Corrosion*, 1997, **53**, p 808–812